Magnetization plateau observed by ultrahigh-field Faraday rotation in the kagome antiferromagnet herbertsmithite

Ryutaro Okuma [1,2,*] Daisuke Nakamura,[1] and Shojiro Takeyama[1]

[1]*Institute for Solid State Physics, University of Tokyo, Kashiwanoha, Chiba 277-8581, Japan*
[2]*Okinawa Institute of Science and Technology Graduate University, Onna-son, Okinawa 904-0495, Japan*

To capture the high-field magnetization process of herbertsmithite [$ZnCu_3(OH)_6Cl_2$], Faraday rotation (FR) measurements were carried out on a single crystal in magnetic fields of up to 190 T. The magnetization data evaluated from the FR angle exhibited a saturation behavior above 150 T at low temperatures, which was attributed to the 1/3 magnetization plateau. The overall behavior of the magnetization process was reproduced by theoretical models based on the nearest-neighbor Heisenberg model. This suggests that herbertsmithite is a proximate kagome antiferromagnet hosting an ideal quantum spin liquid in the ground state. A distinguishing feature is the superlinear magnetization increase, which is in contrast to the Brillouin function-type increase observed by conventional magnetization measurements and indicates a reduced contribution from free spins located at the Zn sites to the FR signal.

Introduction. Geometrically frustrated magnets are of particular interest owing to the possible realization of various exotic quantum states beyond conventional Néel ordering. The quantum spin liquid has been the holy grail of quantum magnetism since the proposal of a nonmagnetic ground state comprising a resonating pattern of singlet pairs in a triangular lattice antiferromagnet by Anderson [1]. A promising platform for realizing a quantum spin liquid is the kagome lattice, which is a two-dimensional net formed by corner-sharing triangular tiling [2–4]. Theoretical investigations into spin-1/2 kagome antiferromagnets have arguably revealed the presence of a quantum spin liquid in the ground state [5,6]. Experimentally, spin-1/2 kagome magnets have been synthesized and some of them show nonmagnetic ground states [7–17].

Among the many candidates for kagome magnets, herbertsmithite $Zn_xCu_{4-x}(OH)_6Cl_2$ ($x \sim 1$) is recognized as one of the closest candidate for the realization of a spin-1/2 Heisenberg kagome antiferromagnet [18]. It has an ordered pyrochlore crystal lattice structure as depicted in Fig. 1. The kagome layer is made up of uniform triangles of Cu^{2+} ions ($3d$ [9], $S = 1/2$), while the nonmagnetic triangular layer comprises Zn^{2+} ions partially replaced by Cu^{2+} substitution [19]. The isotropic nearest-neighbor (NN) interaction in the kagome layer has a strength of 180–300 K, whereas the defect spins in the adjacent triangular layer behave as nearly free spins [20]. Despite such strong interactions, no magnetic order has been observed even at temperatures down to 50 mK [21]. Inelastic neutron-scattering and nuclear magnetic resonance have identified gapless or slightly gapped excitations, which are attributed to deconfined spinons excited from the spin-liquid ground state [22,23].

However, one important issue remains unresolved, namely, the effects of disorder on the ground state of herbertsmithite.

The effects of antisite disorder in herbertsmithite can be divided into two types: one is dilution of the kagome plane by Zn^{2+}, and the other is occupation of the Zn^{2+} site by Jahn-Teller active Cu^{2+}. The former locally breaks the triangles and releases the geometrical frustration. The latter results in the modulation of spin interactions on the kagome plane. Theoretical studies have suggested that in both cases, a certain amount of randomness induces a nonmagnetic state called a valence bond glass [24] or a random singlet state [25,26] in which singlet pairs form a static spatial pattern rather than the resonating valence bond state. In fact, in the absence of a "smoking gun" for the existence of a quantum spin liquid, all the experimental data reported so far can be reproduced by assuming site randomness [24–26].

Here, we present a unique approach to understanding the effects of disorder on the ground state of herbertsmithite by utilizing the characteristic properties of the kagome antiferromagnet subjected to very high magnetic fields. In any magnetic materials, a sufficiently high magnetic field forces all the spins to align along the direction of the field. A Bloch wave of spin flips, called a magnon, is an elementary excitation from such a polarized state. A striking feature of the kagome antiferromagnet is that the magnon does not propagate but resonates inside a hexagon [27]. Below the saturation field, such hexagonal magnons condense into a series of crystalline states in the absence of quenched disorder [27–33]. Experimentally, these can be observed as 1/3, 5/9, and 7/9 magnetization plateaus on the magnetization curve. As the random spin interactions break the local resonances inside the hexagons in the presence of strong randomness, no crystalline phases appear until the magnetization is saturated. Thus, the existence of magnetization plateaus in a kagome antiferromagnet is a useful measure of the proximity to the pristine Heisenberg model without random or additional interactions.

It is expected that magnetic fields higher than 100 T are necessary to observe the first (1/3) magnetization plateau

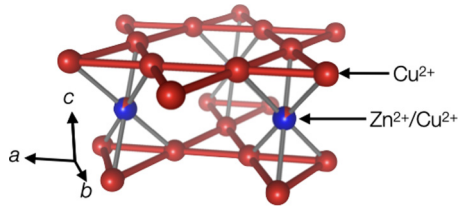---

*ryutaro.okuma@gmail.com

FIG. 1. Magnetic sublattice of herbertsmithite. Red spheres represent Cu^{2+} ions, and red-blue spheres disordered sites with mixed occupancy of Cu^{2+} and Zn^{2+}. Red and grey sticks represent the kagome net intra- and interplane bonds with the disordered sites (Zn^{2+}/Cu^{2+}), respectively.

in herbertsmithite. Precise measurements using the electromagnetic induction method, which has been widely used for magnetization measurements in pulsed magnetic fields, are restricted to measurements below 100 T [34,35]. In contrast, the Faraday rotation (FR) technique is promising for more reliable and noiseless measurements in magnetic fields much higher than 100 T [36,37]. The change in the polarization angle θ_F can be set to be proportional to the magnetization M so that it follows the relation

$$\theta_{\mathrm{F}} = \alpha M d,$$

where α denotes the Verdet constant and d the sample thickness. FR magnetization measurements have been attempted for observing the entire magnetization process in spin-1/2 kagome antiferromagnets at magnetic fields of up to 160 T [38,39]. These precise FR measurements with reduced noise allowed us to identify the presence of a series of magnetization plateaus in Cd-Kapellasite [39].

The single crystals of herbertsmithite used in this study were synthesized by the hydrothermal transport method [40–42]. The composition ratio x in the $Zn_xCu_{4-x}(OH)_6Cl_2$ crystal was determined to be close to 1 by energy dispersive x-ray spectroscopy. The impurity level of the crystal confirmed by a magnetic property measurement system MPMS-3 (Quantum Design) was similar to that reported for $x = 1.0$ [43] as shown in Fig. S1 of the Supplemental Material [45]. The sample was cut along the [101] plane to obtain a hexagonal plate with the dimensions of 1 mm × 1 mm × 0.15 mm. The optically flat crystal was attached to a sapphire substrate and placed into a hand-made miniature liquid-flow-type optical cryostat composed entirely of glass-epoxy thin-wall tubes [44]. A magnetic field with a short-pulsed form (pulse width of 7 μs) was generated by a single-turn coil megagauss generator. A magnetic field of up to around 190 T was applied along the direction perpendicular to the [101] plane of the sample. A 532-nm wavelength laser light source was employed in the FR setup. The photon energy corresponds to 2.3 eV, which is at the higher energy tail of the Cu^{2+} d-d transition spectrum [46]. The angle θ_F was calculated from the intensities of the vertical and horizontal components of the transmitted light through the sample, I_p and I_s, using the formula $\theta_F = a\cos\{(I_p - I_s)/(I_p + I_s)\}$.

Results and discussion. Figure 2 shows the field dependence of the FR signals measured at 6 and 10 K. The temperature pointed out here is the values indicated by the
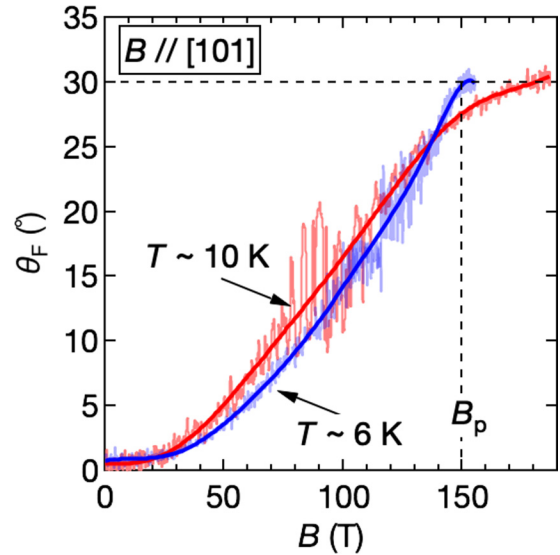

FIG. 2. Evolution of Faraday rotation angle with magnetic field at the temperatures of 6 K (pale blue) and 10 K (pale red). The red and blue solid lines are results of polynomial fitting to the data at 6 and 10 K, respectively. The magnetic field was applied along the [101] axis of the herbertsmithite crystal. The dashed line indicates the position of the magnetization plateau starting from $B_p \sim 150\,\mathrm{T}$.

thermocouple placed adjacent to the sample. The sample temperatures could be larger than these values owing to structural restrictions of the optical cryogenic system [36] and the actual temperature should be considered as 6–8 and 10–18 K, respectively. The drastic noise increases around 120 T at 6 K and 100 T at 10 K are due to a singularity point of θ_F at which I_p vanished and resulted in a substantial decrease of the signal-to-noise ratio. Polynomial fitting was performed and the fits were indicated by solid lines to guide the eye in following the noisy data.

At 6 and 10 K, the rotation angle increment was relatively suppressed below 40 T, above which the rotation angle showed a superlinear increase up to 150 T. Interestingly, at the low-field region, the Brillouin function-type magnetization increment arising from free spins was absent, a fact that stands in contrast with the results obtained by superconducting quantum interference device measurements. This will be discussed later. The magnetization increment was interrupted by a kink at around $B_p \sim 150\,\mathrm{T}$ and saturated above B_p. This indicates the presence of a magnetization plateau with fractional magnetization or the saturation of all spins above B_p.

We first comment on the discrepancy between our results and the magnetization data obtained by the induction method in magnetic fields up to 60 T generated by a nondestructive long pulse magnet [43]. The latter could be interpreted as the magnetization from the kagome plane superimposed with a Brillouin function term due to nearly free interlayer spins. In fact, our sample should show a similar magnetization behavior due to a similar level of impurity concentration.

The discrepancy can be attributed to the site-selectivity of the FR. The FR at the optical wavelength of 532 nm (2.3 eV) arises primarily from the optical transition between the occupied and unoccupied 3d Cu^{2+} orbitals. The optical transition
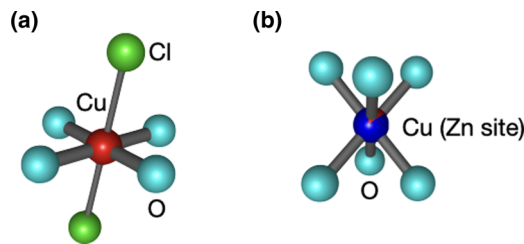
FIG. 3. Local coordination environment of Cu sites. (a) Cu on a kagome plane, and (b) of a disordered site at an interlayer between kagome planes.
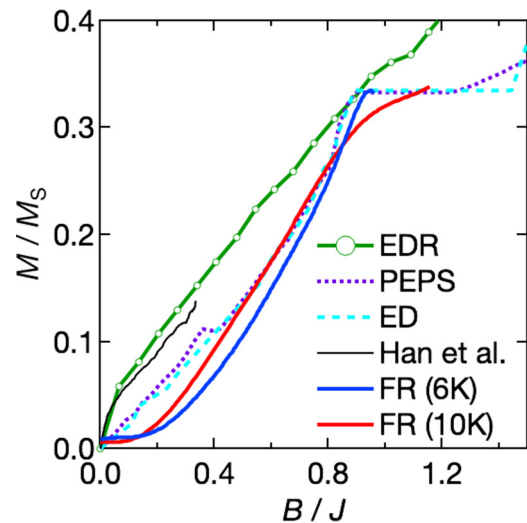

FIG. 4. Comparison of normalized FR data with theoretical calculations: normalized FR data at 6 K (blue) and 10 K (red), magnetization data measured by induction method (thin black) [43], calculation of $S = 1/2$ Heisenberg kagome antiferromagnet by tensor network (PEPS) [42] (purple dotted line) and exact diagonalization (ED) [47] (dashed sky blue), and $S = 1/2$ Heisenberg kagome antiferromagnet with random interaction by exact diagonalization (EDR) [26] (green circle with line). The FR data are normalized by the NN interaction and the FR at the full magnetization, which are assumed to be 250 K and 90°, respectively.

intensity depends on the ligand field splitting and should be sensitive to different chemical environments. Figure 3 illustrates the coordination environment of Cu^{2+} in two different crystallographic sites in herbertsmithite. The copper ion on a kagome plane has octahedral coordination with strong monoclinic distortion and is surrounded by oxygen and chlorine atoms [Fig. 3(a)], whereas the copper ion in a defect position has trigonally distorted octahedral coordination with six surrounding oxygen atoms [Fig. 3(b)]. FR with the photon energy tuned to the ligand field energy splitting of the Cu^{2+} in the kagome plane is reflected predominantly by the magnetization of the kagome plane itself and is less contributed from that of the defect site. This fact is confirmed by subtraction of the free spin contribution from the magnetization data [43], which has resulted in a fairly good agreement with that of the Faraday rotation as is demonstrated in Fig. S2 of the Supplemental Material [45].

The kink around B_p in Fig. 2 evokes the question of whether the magnetization plateau is associated with fractional magnetization or is simply due to the full saturation of the magnetization. The interaction J of herbertsmithite is reported to be around 180–300 K [8,19,20], from which the saturation field is evaluated as $3J = 400$–600. Therefore, the magnetization kink above B_p cannot be caused by full moment saturation but is most likely due to the 1/3 magnetization plateau. This can also be inferred from the theoretical prediction that the plateau starts to appear above $B \sim J$ [28–33,47].

A comparison of various theoretical models and our experiment results is presented in Fig. 4, in which it was assumed that the FR above B_p is the signal corresponding to 1/3 of the full kagome plane magnetization at $J = 250$ K. The theoretical calculations correspond to the spin-1/2 NN Heisenberg kagome antiferromagnet with [26] and without [42,47] disorder. The present FR data match better with the calculated lines modeled without disorder (denoted as PEPS [42] and ED [47] in Fig. 4) than the line with heavy disorder (denoted as EDR [26]). The calculated curve for the latter (EDR) exhibits only a slight anomaly near 1/3 magnetization in contrast to the flat feature observed in the FR signal. The effects of finite temperature and/or existing weak disorder result in the blunt structure at the beginning of the plateau as is observed in the present FR data. The Dzyaloshinskii-Moriya interaction, which is known to exist in this system [48], may also be a possible reason for the blunt structure of the plateau.

The fact that the present FR data are well reproduced by the magnetization curves calculated by models without disorder

has significant implications. The FR data selectively reflect the magnetization from the Cu^{2+} on the kagome planes and disregards the free spins at the defect sites. By choosing the wavelength of the FR light to match a specific intra-atomic transition, it may be possible to obtain the magnetic information of a magnetic ion in a specific environment.

The discussion above thus leads to the important implication that intrinsic herbertsmithite without free-spin defects, if realized, is well described by the pristine NN Heisenberg kagome antiferromagnet.

Conclusion and outlook. The FR data with a specific optical transition indicate a magnetization curve with the tendency to saturate above $B_p \sim 150$ T below 10 K in the spin-1/2 kagome antiferromagnet herbertsmithite. The bending feature above B_p was interpreted as the 1/3 magnetization plateau. The overall magnetization features at up to 190 T were well reproduced by the pristine NN Heisenberg kagome antiferromagnet. These facts indicate that the mineral herbertsmithite, if eliminated from chemical disorder, is close to the ideal Heisenberg kagome antiferromagnet. However, more compelling evidence for crystallization and magnon sublimation in the kagome antiferromagnet, e.g., the 5/9 and 7/9 plateaus and an abrupt jump to moment saturation following the 7/9 plateau, remains to be found. The present experiment is anticipated to be extended to around 500 T by using a state-of-the-art electromagnetic flux-compression megagauss generator [49,50] so that the full saturation moment can be observed.

[1] P. W. Anderson, Mater. Res. Bull. **8**, 153 (1973).

[2] J. N. Reimers and A. J. Berlinsky, Phys. Rev. B **48**, 9539 (1993).

[3] D. A. Huse and A. D. Rutenberg, Phys. Rev. B **45**, 7536(R) (1992).

[4] J. T. Chalker, P. C. W. Holdsworth, and E. F. Shender, Phys. Rev. Lett. **68**, 855 (1992).

[5] S. Yan, D. A. Huse, and S. R. White, Science **332**, 1173 (2011).

[6] H. J. Liao, Z. Y. Xie, J. Chen, Z. Y. Liu, H. D. Xie, R. Z. Huang, B. Normand, and T. Xiang, Phys. Rev. Lett. **118**, 137202 (2017).

[7] Z. Hiroi, M. Hanawa, N. Kobayashi, M. Nohara, H. Takagi, Y. Kato, and M. Takigawa, J. Phys. Soc. Jpn. **70**, 3377 (2001).

[8] M. P. Shores, E. A. Nytko, B. M. Bartlett, and D. G. Nocera, J. Am. Chem. Soc. **127**, 13462 (2005).

[9] K. Morita, M. Yano, T. Ono, H. Tanaka, K. Fujii, H. Uekusa, Y. Narumi, and K. Kindo, J. Phys. Soc. Jpn. **77**, 043707 (2008).

[10] R. H. Colman, C. Ritter, and A. S. Wills, Chem. Mater. **20**, 6897 (2008).

[11] Y. Okamoto, H. Yoshida, and Z. Hiroi, J. Phys. Soc. Jpn. **78**, 033701 (2009).

[12] E. A. Nytko, M. P. Shores, J. S. Helton, and D. G. Nocera, Inorg. Chem. **48**, 7782 (2009).

[13] F. H. Aidoudi, D. W. Aldous, R. J. Goff, A. M. Z. Slawin, J. P. Attfield, R. E. Morris, and P. Lightfoot, Nat. Chem. **3**, 801 (2011).

[14] W. Sun, Y.-X. Huang, S. Nokhrin, Y. Pan, and J.-X. Mi, J. Mater. Chem. C **4**, 8772 (2016).

[15] M. Goto, H. Ueda, C. Michioka, A. Matsuo, K. Kindo, and K. Yoshimura, Phys. Rev. B **94**, 104432 (2016).

[16] H. Yoshida, N. Noguchi, Y. Matsushita, Y. Ishii, Y. Ihara, M. Oda, H. Okabe, S. Yamashita, Y. Nakazawa, A. Takata, T. Kida, Y. Narumi, and M. Hagiwara, J. Phys. Soc. Jpn. **86**, 033704 (2017).

[17] P. Puphal, M. Bolte, D. Sheptyakov, A. Pustogow, K. Kliemt, M. Dressel, M. Baenitz, and C. Krellner, J. Mater. Chem. C **5**, 2629 (2017).

[18] M. R. Norman, Rev. Mod. Phys. **88**, 041002 (2016).

[19] D. E. Freedman, T. H. Han, A. Prodi, P. Müller, Q.-Z. Huang, Y.-S. Chen, S. M. Webb, Y. S. Lee, T. M. McQueen, and D. G. Nocera, J. Am. Chem. Soc. **132**, 16185 (2010).

[20] T.-H. Han, M. R. Norman, J.-J. Wen, J. A. Rodriguez-Rivera, J. S. Helton, C. Broholm, and Y. S. Lee, Phys. Rev. B **94**, 060409(R) (2016).

[21] J. S. Helton, K. Matan, M. P. Shores, E. A. Nytko, B. M. Bartlett, Y. Yoshida, Y. Takano, A. Suslov, Y. Qiu, J.-H. Chung, D. G. Nocera, and Y. S. Lee, Phys. Rev. Lett. **98**, 107204 (2007).

[22] T.-H. Han, J. S. Helton, S. Chu, D. G. Nocera, J. A. Rodriguez-Rivera, C. Broholm, and Y. S. Lee, Nature (London) **492**, 406 (2012).

[23] M. Fu, T. Imai, T.-H. Han, and Y. S. Lee, Science **350**, 655 (2015).

[24] R. R. P. Singh, Phys. Rev. Lett. **104**, 177203 (2010).

[25] H. Kawamura, K. Watanabe, and T. Shimokawa, J. Phys. Soc. Jpn. **83**, 103704 (2014).

[26] T. Shimokawa, K. Watanabe, and H. Kawamura, Phys. Rev. B **92**, 134407 (2015).

[27] J. Schulenburg, A. Honecker, J. Schnack, J. Richter, and H. J. Schmidt, Phys. Rev. Lett. **88**, 167207 (2002).

[28] K. Hida, J. Phys. Soc. Jpn. **70**, 3673 (2001).

[29] S. Nishimoto, N. Shibata, and C. Hotta, Nat. Commun. **4**, 2287 (2013).

[30] S. Capponi, O. Derzhko, A. Honecker, A. M. Läuchli, and J. Richter, Phys. Rev. B **88**, 144416 (2013).

[31] T. Picot, M. Ziegler, R. Orús, and D. Poilblanc, Phys. Rev. B **93**, 060407(R) (2016).

[32] D. Huerga, S. Capponi, J. Dukelsky, and G. Ortiz, Phys. Rev. B **94**, 165124 (2016).

[33] X. Chen, S.-J. Ran, T. Liu, C. Peng, Y.-Z. Huang, and G. Su, Sci. Bull. **63**, 1545 (2018).

[34] S. Takeyama, R. Sakakura, Y. H. Matsuda, A. Miyata, and M. Tokunaga, J. Phys. Soc. Jpn. **81**, 014702 (2012).

[35] Y. Okamoto, D. Nakamura, A. Miyake, S. Takeyama, M. Tokunaga, A. Matsuo, K. Kindo, and Z. Hiroi, Phys. Rev. B **95**, 134438 (2017).

[36] E. Kojima, A. Miyata, S. Miyabe, S. Takeyama, H. Ueda, and Y. Ueda, Phys. Rev. B **77**, 212408 (2008).

[37] A. Miyata, H. Ueda, Y. Ueda, H. Sawabe, and S. Takeyama, Phys. Rev. Lett. **107**, 207203 (2011).

[38] D. Nakamura, T. Yamashita, H. Ishikawa, Z. Hiroi, and S. Takeyama, Phys. Rev. B **98**, 020404(R) (2018).

[39] R. Okuma, D. Nakamura, T. Okubo, A. Miyake, A. Matsuo, K. Kindo, M. Tokunaga, N. Kawashima, S. Takeyama, and Z. Hiroi, Nat. Commun. **10**, 1229 (2019).

[40] T. H. Han, J. S. Helton, S. Chu, A. Prodi, D. K. Singh, C. Mazzoli, P. Müller, D. G. Nocera, and Y. S. Lee, Phys. Rev. B **83**, 100402(R) (2011).

[41] S. Chu, P. Muller, D. G. Nocera, and Y. S. Lee, Appl. Phys. Lett. **98**, 092508 (2011).

[42] R. Okuma, T. Yajima, D. Nishio-Hamane, T. Okubo, and Z. Hiroi, Phys. Rev. B **95**, 094427 (2017).

[43] T.-H. Han, R. Chisnell, C. J. Bonnoit, D. E. Freedman, V. S. Zapf, N. Harrison, D. G. Nocera, Y. Takano, and Y. S. Lee, arXiv:1402.2693.

[44] S. Takeyama, M. Kobayashi, A. Matsui, K. Mizuno, and N. Miura, in *High Magnetic Fields in Semiconductor Physics*, edited by G. Landwehr, Springer Series in Solid State Physics Vol. 71 (Springer, Berlin, 1987), p. 555.

[45] See Supplemental Material at http://link.aps.org/supplemental/10.1103/PhysRevB.102.104429 for concentration of impurity in the crystal used in our study and comparison of bulk magnetization and faraday rotation angle.

[46] A. Pustogow, Y. Li, I. Voloshenko, P. Puphal, C. Krellner, I. I. Mazin, M. Dressel, and R. Valentí, Phys. Rev. B **96**, 241114(R) (2017).

[47] H. Nakano and T. Sakai, J. Phys. Soc. Jpn. **87**, 063706 (2018).

[48] A. Zorko, S. Nellutla, J. van Tol, L. C. Brunel, F. Bert, F. Duc, J.-C. Trombe, M. A. de Vries, A. Harrison, and P. Mendels, Phys. Rev. Lett. **101**, 026405 (2008).

[49] A. Miyata, H. Ueda, Y. Ueda, Y. Motome, N. Shannon, K. Penc, and S. Takeyama, J. Phys. Soc. Jpn. **80**, 074709 (2011).

[50] D. Nakamura, A. Ikeda, H. Sawabe, Y. H. Matsuda, and S. Takeyama, Rev. Sci. Instrum. **89**, 095106 (2018).